Cao et al. Nanoscale Research Letters (2015) 10:251
DOI 10.1186/s11671-015-0952-x

Nanoscale Research Letters
a SpringerOpen Journal

NANO EXPRESS Open Access

Magnetically Separable Fe_3O_4/AgBr Hybrid Materials: Highly Efficient Photocatalytic Activity and Good Stability

Yuhui Cao[1], Chen Li[1], Junli Li[1], Qiuye Li[1,2*] and Jianjun Yang[1,2*]

Abstract

Magnetically separable Fe_3O_4/AgBr hybrid materials with highly efficient photocatalytic activity were prepared by the precipitation method. All of them exhibited much higher photocatalytic activity than the pure AgBr in photodegradation of methyl orange (MO) under visible light irradiation. When the loading amount of Fe_3O_4 was 0.5 %, the hybrid materials displayed the highest photocatalytic activity, and the degradation yield of MO reached 85 % within 12 min. Silver halide often suffers serious photo-corrosion, while the stability of the Fe_3O_4/AgBr hybrid materials improved apparently than the pure AgBr. Furthermore, depositing Fe_3O_4 onto the surface of AgBr could facilitate the electron transfer and thereby leading to the elevated photocatalytic activity. The morphology, phase structure, and optical properties of the composites were characterized by scanning electron microscopy (SEM), X-ray diffraction (XRD), UV–visible diffuse reflectance spectra (UV–vis DRS), and photoluminescence (PL) techniques.

Keywords: AgBr; Fe_3O_4; Magnetic separation; Visible light; Photocatalysis

Background

Up to now, most of the silver oxide and silver halide have attracted much attention because of their strong visible light absorption performance [1–7]. Particularly, AgBr, which has a band gap of 2.6 eV, is well known as a photosensitive material and has been extensively applied to photographic films, which demonstrated excellent performance in degradation of dye pollutants and decomposition of water [8–10]. For example, Ag/AgBr/TiO_2 [11], Ag–AgBr/TiO_2/RGO [12], AgBr(I)@Ag [13], Fe(III)/AgBr [14], and Ag/AgBr/ZnO [15] have been successfully fabricated by diverse techniques, and their novel and unique photocatalytic properties have been extensively explored.

For the nanosized or microsized photocatalysts, effective separation from the mixed system and recycle using are important problems to restrain their real applications [16, 17]. Immobilizing catalysts on magnetic substrates by feasible methods is proven to be an effective approach for removing and recycling particles [18–21]. Moreover, Fe_3O_4 has excellent conductivity, so it could act as an electron transfer channel and acceptor, which could suppress the photo-generated carrier recombination. For instance, Ye et al. reported that the hierarchical core–shell-structured Fe_3O_4/WO_3 has a more effective photoconversion capability than pure WO_3 or Fe_3O_4 [22]. The Ag halides such as AgBr and AgI are photoactive to visible light. When they were immobilized on SiO_2@Fe_3O_4 magnetic supports, they exhibited faster degradation rates for 4-chlorophenol than N-TiO_2 [23]. However, the Ag halides were easily photoreduced and losed their stability quickly.

The motivation of the present research originated from the idea that Fe_3O_4 has high conductivity and its CB level (1 V vs. NHE) makes it become a good candidate for coupling with AgBr. Based on the above reason, we prospect their combination could improve the photocatalytic performance by enhancing charge transport. Herein, conductive Fe_3O_4 particles and visible light active AgBr were coupled together to prepare the magnetically recyclable Fe_3O_4/AgBr composites with visible light activity. Studies of their photocatalytic performance in the decomposition of methyl orange (MO) indicated that Fe_3O_4/AgBr photocatalysts exhibited excellent catalytic activity under visible

* Correspondence: qiuyeli@henu.edu.cn; yangjianjun@henu.edu.cn
[1]Key Laboratory for Special Functional Materials of Ministry of Education, Henan University, Kaifeng 475004, China
[2]Collaborative Innovation Center of Nano Functional Materials and Applications, Henan Province, China
Full list of author information is available at the end of the article

light illumination. Meanwhile, the stability of AgBr was improved when it was coupled with Fe_3O_4.

Methods

Preparation of the Photocatalyst

Synthesis of Fe_3O_4 Nanospheres

The Fe_3O_4 nanospheres were prepared according to the literature reported previously [24]. In a typical synthesis, 0.5 g of 1 g $FeCl_3 \cdot 3H_2O$, 3.0 g NaAc, and 10 mL oleic acid were added to 30 mL ethylene glycol into a three-necked flask, and then a red solution was formed. The mixture was stirred vigorously at 50 °C for 20 min until all reagents were dissolved completely. Then, the mixture was transferred into a Teflon-lined autoclave and heated at 200 °C for 20 h. The products were cooled down to room temperature, washed with ethanol for several times, and dried under vacuum to give a black solid.

Synthesis of Fe_3O_4/AgBr Hybrid Materials

Fe_3O_4 nanospheres (0.01 g) were dispersed in 20 mL deionized water and then ultrasonically dispersed evenly. $AgNO_3$ (1.18 g) was added into the solution, and then NaBr (0.1 mol/L) was added dropwise slowly. The resulting suspensions were filtered, washed several times with distilled water, and finally dried in vacuum. Different Fe_3O_4/AgBr samples were obtained by adjusting the mass ratio of Fe_3O_4 and AgBr, and the sample was denoted as Fe_3O_4/AgBr-x (x means the percentage of Fe_3O_4).

Characterization

X-ray diffraction (XRD) patterns were measured on an X'Pert Philips diffractometer (Cu Kα radiation, 2θ range 10°–90°, step size 0.08°, accelerating voltage 40 kV, applied current 40 mA). The morphology of the samples was taken on a Hitachi S-4800 scanning electron microscope (SEM). UV–visible diffuse reflectance spectra (UV–vis DRS) were obtained on a Shimadzu U-3010 spectrometer, using $BaSO_4$ as a reference. The photoluminescence (PL) spectra were recorded on a F-7000 FL spectrophotometer.

Evaluation of the Photocatalytic Activity

MO was selected as the model pollutant to evaluate the photocatalytic activity of the Fe_3O_4/AgBr hybrid materials. In a typical experiment, 0.1 g of the photocatalyst was put into a 120 mL quartz reactor containing 100 mL MO aqueous suspension (20 mg/L, pH = 7). Prior to irradiation, the suspension was magnetically stirred in the dark for 30 min to establish an adsorption–desorption equilibrium. A 300-W Xe arc lamp with a 420 cutoff filter was used as the light source ($\lambda \geq 420$ nm, $I_{420} = 8.0$ mW/cm^2). At 2-min intervals, 5 mL of the suspension was collected and centrifuged for 3 min to remove the catalyst particulates for analysis. The residual MO concentration was detected at 464 nm using a UV–vis spectrophotometer (722, Shanghai Jingke Instrument Plant, China).

Results and Discussion

Phase Structure and Morphology of the Samples

Figure 1a shows that the size of Fe_3O_4 nanospheres was about 100 ~ 200 nm. The surface of Fe_3O_4 particles was rough, and each magnetic microsphere was constructed with many small magnetic grains. From Fig. 1b, we can clearly see that the obtained AgBr particles by the precipitation method easily agglomerate to large particles and their size was more than 300 nm. Figure 1c displays that when Fe_3O_4 was coupled with AgBr, the particle size of the composite increased apparently than the pure AgBr particles. The magnetic property of the surface Fe_3O_4 would result in the agglomeration of the particles. The EDS spectrum of Fe_3O_4/AgBr-0.5 hybrid materials indicates that the atomic ratio of Fe and Ag is approximately 1:134, which is a little larger than the designed value.

Figure 2 shows the typical XRD patterns of the as-prepared Fe_3O_4/AgBr hybrid materials with different Fe_3O_4 contents, which matched well with those of Fe_3O_4 (magnetite, JCPDS 85-1436) [22]. The diffraction peaks of pure AgBr at 26.8°, 30.9°, 44.3°, 55.0°, and 64.5° were assigned to the (111), (200), (220), (222), and (400) crystal planes of AgBr (JCPDS 06-4308) [14]. With increasing Fe_3O_4 content, no characteristic peaks were ascribed to Fe_3O_4 emerging with AgBr phase, which should be due to the lower content of Fe_3O_4.

Optical Properties of the Photocatalysts

The UV–vis spectra of Fe_3O_4/AgBr hybrid materials are illustrated in Fig. 3. The pure Fe_3O_4 particles show strong absorption both in ultraviolet and visible light regions, which may be attributed to its small band gap. The absorption band edge of AgBr was about 470 nm, so the calculated band gap was 2.64 eV. AgBr was often used as a good visible light sensitizer because it exhibited a strong absorption in the visible light. After loading Fe_3O_4 on AgBr particles, the visible light absorption increased significantly. And as the increase with the loading content of Fe_3O_4, the visible absorption of the composites enhanced gradually, indicating that the existence of Fe_3O_4 could promote visible light absorption effectively.

Photocatalytic Activity for MO Degradation on Fe_3O_4/AgBr Hybrid Materials

The photocatalytic performances of the photocatalysts were evaluated by photoinduced decolorization of MO aqueous solution, as shown in Fig. 4. Prior to irradiation, the mixed solution of MO and photocatalyst was kept in the dark for 30 min to obtain an adsorption/desorption

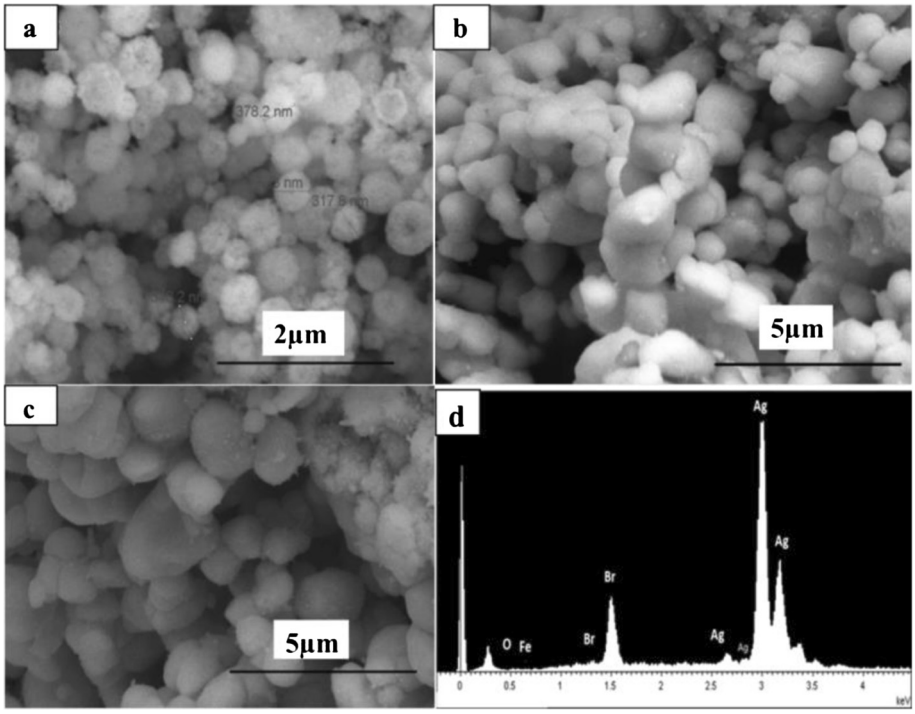

Fig. 1 SEM images of the Fe_3O_4/AgBr hybrid materials obtained. **a** Fe_3O_4. **b** AgBr. **c** Fe_3O_4/AgBr-0.5. **d** EDS images of Fe_3O_4/AgBr-0.5

equilibrium. For comparison, the photocatalytic activity of the pure AgBr was tested and the degradation yield reached approximately 55 % in 12 min. When Fe_3O_4 nanospheres were loaded on AgBr particles, the photocatalytic activity increased apparently than the pure AgBr. The photocatalytic mechanism of Fe_3O_4/AgBr composites for MO degradation under visible light is illustrated in Fig. 5. The CB level of Fe_3O_4 (1 V vs. NHE) is much lower than that of AgBr (−1.1 V vs. NHE) [22–25], so the photo-excited electrons on the conduction band (CB) of AgBr can transfer to the CB of Fe_3O_4. And the conductivity of Fe_3O_4 is as high as 1.9×10^6 S m^{-1}; the electrons on Fe_3O_4 particles would transfer out quickly and react with the surface pollutants. Meanwhile, Ag nanoparticles on the surface of AgBr can act as electron capture traps to improve the separation efficiency of the charge carriers and thereby improving the photocatalytic efficiency. These should be the main reason for the enhancement of the photocatalytic

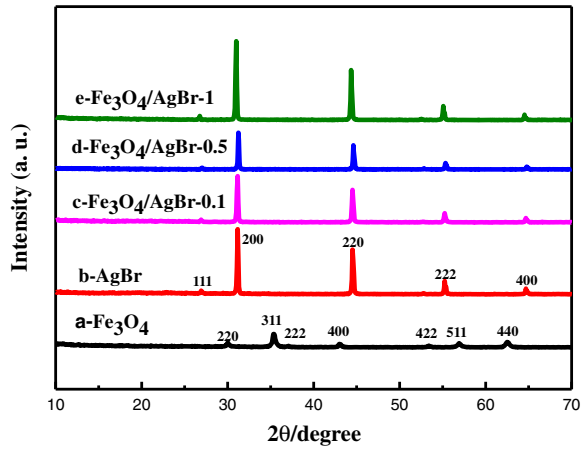

Fig. 2 XRD pattern of the photocatalysts obtained. (**a**) Fe_3O_4. (**b**) AgBr. (**c**) Fe_3O_4/AgBr-0.1. (**d**) Fe_3O_4/AgBr-0.5. (**e**) Fe_3O_4/AgBr-1

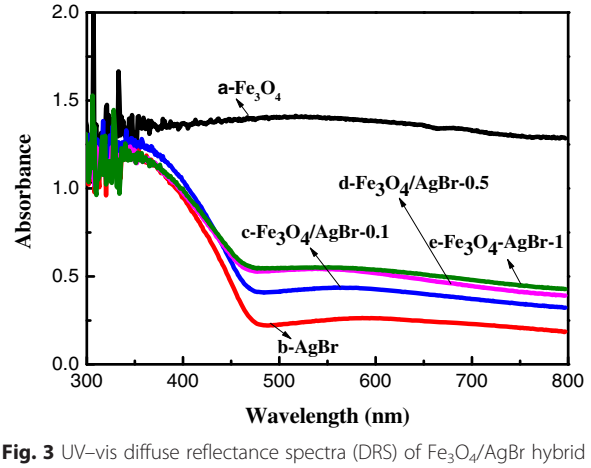

Fig. 3 UV–vis diffuse reflectance spectra (DRS) of Fe_3O_4/AgBr hybrid materials obtained. (**a**) Fe_3O_4. (**b**) AgBr. (**c**) Fe_3O_4/AgBr-0.1. (**d**) Fe_3O_4/AgBr-0.5. (**e**) Fe_3O_4/AgBr-1

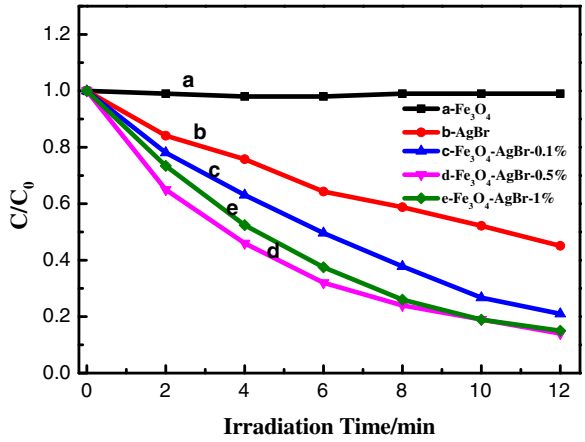

Fig. 4 Visible light responded photodegradation of MO on the series of photocatalysts obtained. (**a**) Fe_3O_4. (**b**) AgBr. (**c**) Fe_3O_4/AgBr-0.1. (**d**) Fe_3O_4/AgBr-0.5. (**e**) Fe_3O_4/AgBr-1

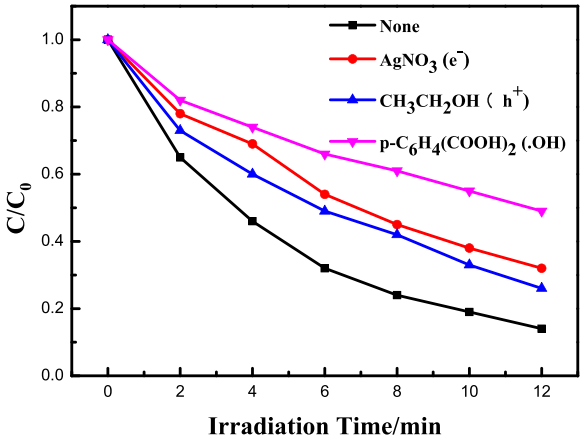

Fig. 6 Detection of the active species of electrons, holes, and hydroxyl radicals

activity for Fe_3O_4/AgBr composites. In addition, the loading amount of Fe_3O_4 particles has an effect on the activity of the composites. The sample Fe_3O_4/AgBr-0.5 has the best photocatalytic activity; the degradation yield of MO reached nearly 85 % within 12 min. In order to clarify the reasons for this result, the active species in photodegradation process of MO were detected. Methanol, silver nitrate, and terephthalic acid solution were added into MO dye solution to capture electrons, holes, and · OH, respectively. As can be seen from Fig. 6, when the active species of electrons, holes, and · OH were captured, the degradation yield of MO decreased from 85 % to 68 %, 74 %, and 51 %, respectively. That indicated · OH and electrons played more important roles comparing the holes in the photodegradation of MO.

As well known, AgBr is not stable, and it often suffers photo-corrosion. So, the stability of AgBr and Fe_3O_4/AgBr-0.5 was evaluated. As shown in Fig. 7, the photocatalytic activity on the pure AgBr decreased sharply in the consecutive three cycles. The degradation yield of MO on the pure AgBr particles in the tree cycles was 0.52, 0.33, and 0.12, respectively. The photo-excited electrons on AgBr would reduce Ag^+ to the metallic Ag, and the small Ag nanoparticles would cover on the surface of AgBr. And the surface Ag nanoparticles would prohibit the photo-absorption of the inner AgBr. When the amount of Ag was enough, the photo-excitation of the inner AgBr would be hold back, and as a result, the photocatalytic activity decreased remarkably as the reaction proceeding. However, for the Fe_3O_4/AgBr hybrid

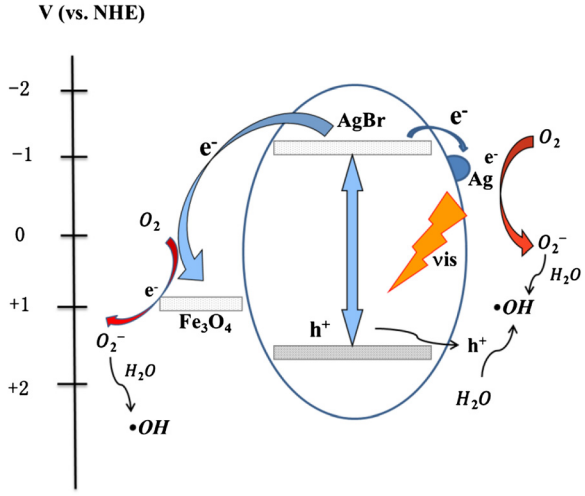

Fig. 5 Photocatalytic mechanism of MO degradation on Fe_3O_4/AgBr hybrid materials under visible light illumination

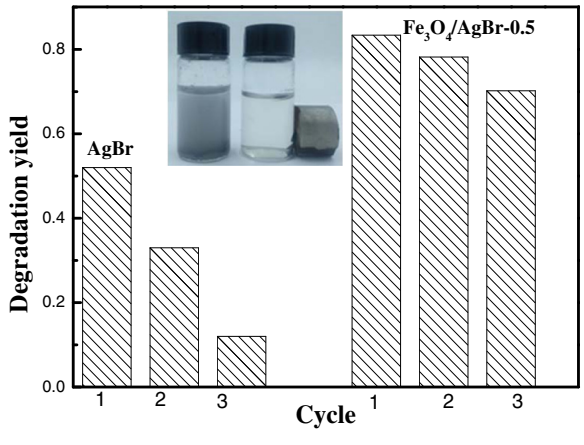

Fig. 7 The stability of the pure AgBr and Fe_3O_4/AgBr-0.5 hybrid materials on MO photodegradation in the consecutive three cycles. The inset shows that Fe_3O_4/AgBr-0.5 composites have a certain magnetic response to an applied magnetic field

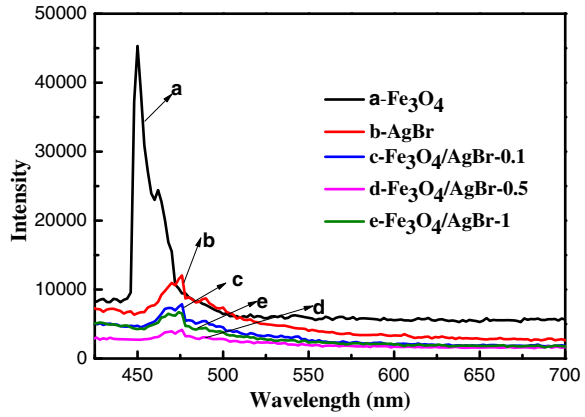

Fig. 8 Photoluminescence (PL) spectra obtained. (**a**) Fe_3O_4. (**b**) AgBr. (**c**) Fe_3O_4/AgBr-0.1. (**d**) Fe_3O_4/AgBr-0.5. (**e**) Fe_3O_4/AgBr-1

materials, the stability was much better. The degradation yield of MO on Fe_3O_4/AgBr composites was 0.83, 0.78, and 0.71 in the consecutive cycles, respectively. The Fe_3O_4 particles on the surface could transfer the photo-excited electrons out quickly, which inhibit the self-reduction of AgBr. So, the long-term stability of Fe_3O_4/AgBr composites was obtained than the pure AgBr. In the photocatalytic application, effective recycling of catalyst is very important. Thanks to the existence of Fe_3O_4, the catalyst has magnetism, which is favorable for recycling. As shown in the inset of Fig. 7, Fe_3O_4/AgBr-0.5 composites could be easily separated from the suspension by an external magnetic field. As expected, the as-prepared Fe_3O_4/AgBr composites exhibited a certain magnetic response.

Photoluminescence of the Series of Photocatalysts

The fluorescence spectrum can provide much more information about carrier capture, migration, conversion, separation, etc., so it has been used for measuring the separation of the photo-generated electron–hole pairs [26]. The emission signals in the fluorescence spectrum are mainly from the recombination of the photo-generated electron–hole pairs, and the lower fluorescence intensity often implies the higher separation efficiency of the charge carriers. Figure 8 shows the fluorescence spectra of the samples in a wavelength range of 400–700 nm. It can be seen that the peaks were similar except Fe_3O_4. No characteristic peaks were ascribed to Fe_3O_4 emerging with Fe_3O_4/AgBr composites, which should be due to the lower content of Fe_3O_4. Moreover, Fig. 8 also shows a decrease in emission intensity from AgBr to Fe_3O_4/AgBr samples, indicating that an appropriate amount of Fe_3O_4 could significantly reduce the recombination rate of photo-generated electrons and holes of AgBr. The PL intensity of the Fe_3O_4/AgBr-0.5 sample was the lowest, which indicated that the separation efficiency of charge carriers was the highest. That was in accord with the photocatalytic activity result very well.

Conclusions

Fe_3O_4/AgBr hybrid materials with high photocatalytic efficiency under visible light were prepared through the precipitation method. The Fe_3O_4/AgBr samples showed much higher photocatalytic activity than the pure AgBr, which was due to the matched band structure of two components and the higher conductivity of Fe_3O_4. When the loading amount of Fe_3O_4 was 0.5 %, the highest photoactivity was obtained, and the degradation yield of MO reached 85 % within 12 min. The PL spectra indicated that Fe_3O_4/AgBr hybrid materials had the higher separation efficiency of the photo-excited charge carriers, and that was in accordance with the photocatalytic activity very well. In addition, the stability of Fe_3O_4/AgBr composites was improved comparing with the pure AgBr. The photo-excited electrons would transfer out quickly from the surface Fe_3O_4, so the self-reduction of AgBr to metallic Ag was prohibited, and as a result, the long-term stability of Fe_3O_4/AgBr was obtained.

Competing interests

The authors declare that they have no competing interests.

Authors' contributions

YC carried out the total experiment and wrote the manuscript. CL and JL participated in the data analysis. QL supervised the project. JY provided the facilities and discussions related to them. All authors read and approved the final manuscript.

Acknowledgements

The authors gratefully acknowledge the support of the National Science Foundation of China (Nos. 21103042 and 21471047), Program for Science & Technology Innovation Talents in University of Henan Province (No. 15HASTIT043), and the Natural Science Foundation of Henan University (No. 2012YBZR001).

Received: 11 March 2015 Accepted: 21 May 2015
Published online: 03 June 2015

References

1. Li GQ, Wang DF, Zou ZG, Ye JH. Enhancement of visible-light photocatalytic activity of $Ag_{0.7}Na_{0.3}NbO_3$ modified by a platinum complex. J Phys Chem C. 2008;112:20329–33.
2. Ouyang SX, Li ZS, Ouyang Z, Yu T, Ye JH, Zou ZG. Correlation of crystal structures, electronic structures, and photocatalytic properties in a series of Ag-based oxides: $AgAlO_2$, $AgCrO_2$, and Ag_2CrO_4. J Phys Chem C. 2008;112:3134–41.
3. Kako T, Kikugawa N, Ye JH. Photocatalytic activities of $AgSbO_3$ under visible light irradiation. Catal Today. 2008;131:197–202.
4. Xu M, Han L, Dong SJ. Facile fabrication of highly efficient g-C_3N_4/Ag_2O heterostructured photocatalysts with enhanced visible-light photocatalytic activity. ACS Appl Mater Interfaces. 2013;5:12533–40.
5. Wang P, Huang BB, Zhang XY, Qin XY, Jin H, Dai Y, et al. Highly efficient visible-light plasmonic photocatalyst Ag@AgBr. Chem-A Eur J. 2009;15:1821–4.
6. Li YZ, Zhang H, Guo ZM, Han JJ, Zhao XJ, Zhao QN, et al. Highly efficient visible-light-induced photocatalytic activity of nanostructured AgI/TiO_2 photocatalyst. Langmuir. 2008;24:8351–7.
7. Li MC, Yu H, Huang R, Bai F, Trevor M, Song DD, et al. Facile one-pot synthesis of flower-like AgCl microstructures and enhancing of visible light photocatalysis. Nanoscale Res Lett. 2013;8:442–8.

8. Wang P, Huang BB, Zhang QQ, Zhang XY, Qin XY, Dai Y, et al. Highly efficient visible light plasmonic photocatalyst Ag@Ag (Br, I). Chem-A Eur J. 2010;16:10042–7.
9. Kuai L, Geng BY, Chen XT, Zhao YY, Luo YC. Facile subsequently light-induced route to highly efficient and stable sunlight-driven Ag-AgBr plasmonic photocatalyst. Langmuir. 2010;26:18723–7.
10. Tian GH, Chen YJ, Bao HL, Meng XY, Pan K, Zhou W, et al. Controlled synthesis of thorny anatase TiO_2 tubes for construction of Ag–AgBr/TiO_2 composites as highly efficient simulated solar-light photocatalyst. J Mater Chem. 2012;22:2081–8.
11. Hu C, Lan YQ, Qu JH, Hu XX, Wang AM. Ag/AgBr/TiO_2 visible light photocatalyst for destruction of azodyes and bacteria. J Phys Chem B. 2006;110:4066–72.
12. Wang PH, Tang YX, Dong ZL, Chen Z, Lim T-T. Ag–AgBr/TiO_2/RGO nanocomposite for visible-light photocatalytic degradation of penicillin. J Mater Chem A. 2013;1:4718–27.
13. Yang F, Tian BZ, Zhang JL, Xiong TQ, Wang TT. Preparation, characterization, and photocatalytic activity of porous AgBr@Ag and AgBrI@Ag plasmonic photocatalysts. Appl Surf Sci. 2014;292:256–61.
14. Yu HG, Xu LL, Wang P, Wang XF, Yu JG. Enhanced photoinduced stability and photocatalytic activity of AgBr photocatalyst by surface modification of Fe(III) cocatalyst. Appl Catal B Environ. 2014;144:75–82.
15. Shi L, Liang L, Ma J, Meng YN, Zhong SF, Wang FX, et al. Highly efficient visible light-driven Ag/AgBr/ZnO composite photocatalyst for degrading rhodamine B. Ceram Int. 2014;40:3495–502.
16. Linley S, Leshuk T, Gu FX. Magnetically separable water treatment technologies and their role in future advanced water treatment: a patent review. Clean-Soil Air Water. 2013;41:1152–6.
17. Polshettiwar V, Luque R, Fihri A, Zhu HB, Bouhrara M, Basset J-M. Magnetically recoverable nanocatalysts. Cheml Rev. 2011;111:3036–75.
18. Xu X, Shen XP, Zhu GX, Jing LQ, Liu XS, Chen KM. Magnetically recoverable Bi_2WO_6-Fe_3O_4 composite photocatalysts: fabrication and photocatalytic activity. Chem Eng J. 2012;200–202:521–31.
19. Zhang L, Wang WZ, Sun SM, Sun YY, Gao EP, Zhang ZJ. Elimination of BPA endocrine disruptor by magnetic BiOBr@SiO_2@Fe_3O_4 photocatalyst. Appl Catal B Environ. 2014;148–149:164–9.
20. Zhang L, Wang WZ, Zhou L, Shang M, Sun SM. Fe_3O_4 coupled BiOCl: a highly efficient magnetic photocatalyst. Appl Catal B Environ. 2009;90:458–62.
21. Liu HF, Jia ZG, Ji SF, Zheng YY, Li M, Yang H. Synthesis of TiO_2/SiO_2@Fe_3O_4 magnetic microspheres and their properties of photocatalytic degradation dyestuff. Catal Today. 2011;175:293–8.
22. Xi GC, Yue B, Cao JY, Ye JH. Fe_3O_4/WO_3 hierarchical coreshell structure: high-performance and recyclable visible-light photocatalysis. Chem-A Eur J. 2011;17:5145–54.
23. Guo J-F, Ma BW, Yin AY, Fan KN, Dai W-L. Photodegradation of rhodamine B and 4-chlorophenol using plasmonic photocatalyst of Ag–AgI/Fe_3O_4@SiO_2 magnetic nanoparticle under visible light irradiation. Appl Catal B Environ. 2011;101:580–6.
24. Xing YY, Li R, Li QY, Yang JJ. A new method of preparation of AgBr/TiO_2 composites and investigation of their photocatalytic activity. J Nanopart Res. 2012;14:1284–8.
25. Zhang LS, Wong K-H, Chen ZG, Yu JC, Zhao JC, Hu C, et al. AgBr-Ag-Bi_2WO_6 nanojunction system: a novel and efficient photocatalyst with double visible-light active components. Appl Catal A-Gen. 2009;363:221–9.
26. Yu JC, Yu JG, Ho WK, Jiang ZT, Zhang LZ. Effects of F^- doping on the photocatalytic activity and microstructures of nanocrystalline TiO_2 powders. Chem Mater. 2002;14:3808–16.